The Broad-Spectrum Antiviral Compound ST-669 Restricts Chlamydial Inclusion Development and Bacterial Growth and Localizes to Host Cell Lipid Droplets within Treated Cells

Citation	Sandoz, K. M., Valiant, W. G., Eriksen, S. G., Hruby, D. E., Allen, R. D., & Rockey, D. D. (2014). The broad spectrum antiviral compound ST-669 restricts Chlamydial inclusion development and bacterial growth and localizes to host cell lipid droplets within treated cells. Antimicrobial Agents and Chemotherapy, 58(7), 3860-3866. doi:10.1128/AAC.02064-13
DOI	10.1128/AAC.02064-13
Publisher	American Meteorological Society
Version	Version of Record
Terms of Use	http://cdss.library.oregonstate.edu/sa-termsofuse

AAC
Journals.ASM.org

The Broad-Spectrum Antiviral Compound ST-669 Restricts Chlamydial Inclusion Development and Bacterial Growth and Localizes to Host Cell Lipid Droplets within Treated Cells

Kelsi M. Sandoz,[a]* William G. Valiant,[a] Steven G. Eriksen,[a] Dennis E. Hruby,[b] Robert D. Allen III,[b]* Daniel D. Rockey[a]

Department of Biomedical Sciences, Oregon State University, Corvallis, Oregon, USA[a]; Siga Technologies, Inc., Corvallis, Oregon, USA[b]

Novel broad-spectrum antimicrobials are a critical component of a strategy for combating antibiotic-resistant pathogens. In this study, we explored the activity of the broad-spectrum antiviral compound ST-669 for activity against different intracellular bacteria and began a characterization of its mechanism of antimicrobial action. ST-669 inhibits the growth of three different species of chlamydia and the intracellular bacterium *Coxiella burnetii* in Vero and HeLa cells but not in McCoy (murine) cells. The anti-chlamydial and anti-*C. burnetii* activity spectrum was consistent with those observed for tested viruses, suggesting a common mechanism of action. Cycloheximide treatment in the presence of ST-669 abrogated the inhibitory effect, demonstrating that eukaryotic protein synthesis is required for tested activity. Immunofluorescence microscopy demonstrated that different chlamydiae grow atypically in the presence of ST-669, in a manner that suggests the compound affects inclusion formation and organization. Microscopic analysis of cells treated with a fluorescent derivative of ST-669 demonstrated that the compound localized to host cell lipid droplets but not to other organelles or the host cytosol. These results demonstrate that ST-669 affects intracellular growth in a host-cell-dependent manner and interrupts proper development of chlamydial inclusions, possibly through a lipid droplet-dependent process.

Chlamydiae infect a broad range of animal species and cause disease in a variety of tissues. In humans, sexually transmitted *Chlamydia trachomatis* is the most common reportable infection in the United States, and the pathogen is a leading cause of preventable blindness worldwide (1). These obligately intracellular bacteria attach and enter host cells as nonreplicating elementary bodies (EB) that differentiate into metabolically active reticulate bodies (RB) once inside the cell (2). All chlamydial growth and development occurs within an intracellular parasitophorous vacuole termed the inclusion. Chlamydiae recruit and modify Golgi body-derived vesicles to initiate inclusion growth and transport host-derived phospholipids, cholesterol, and fatty acids into the inclusion and bacterial membranes (3–9). Lipids are trafficked from the site of synthesis to various destinations within the cell, via either a vesicle-dependent or a vesicle-independent pathway. However, recently published data suggest that chlamydiae utilize an additional pathway for recruitment of lipids to facilitate membrane development during chlamydial growth. *Chlamydia* spp. secrete proteins into the cytoplasm that localize to the surface of lipid droplets (LDs) and translocate the LDs across the inclusion membrane. At least 40% of chlamydial phospholipid content is host derived, and the blocking of LD formation or phospholipid uptake with chemical inhibitors has a dramatic effect on chlamydial growth (4, 10, 11). Collectively, this provides evidence for the use of an alternate, non-vesicle-mediated source of host-derived phospholipids by chlamydiae and demonstrates the importance of lipid trafficking and lipid acquisition for chlamydial growth and development.

LDs are lipid storage organelles encased in a phospholipid monolayer, making them unique from other intracellular compartments. They are prominent structures in adipocytes, mammary, and liver cells but can be abundant in other cell types as well (12). LDs function in energy metabolism, steroid biosynthesis, and coordination of the immune response and serve as a reservoir of membrane lipid precursors (13–15). They are targeted by both bacteria and viruses as a source of cholesterol, phospholipid, or fatty acids (16). Hepatitis C virus and dengue virus are among several viruses that have been shown to utilize host LDs during their life cycle (17, 18). A diverse and increasing number of intracellular organisms rely upon LD organelles during intracellular growth (19–21).

ST-669 is one of several acyl thiourea-based broad-spectrum antiviral molecules that were identified and characterized by researchers at Siga Technologies in a high-throughput screen of a chemically defined compound library (22). The compound has a high selective index and inhibits a wide variety of viruses, including dengue, human immunodeficiency, and vaccinia viruses at submillimolar concentrations. The broad-spectrum activity of this compound and the specificity to primate cell lines suggested that it may affect a host cell process that intersects in some way with the growth and development of a wide range of intracellular pathogens. For this reason, it was hypothesized that ST-669 may also delay the growth and development of intracellular bacteria such as *Chlamydia* spp. and *Coxiella burnetii*. To explore this possibility, we evaluated ST-669 against a variety of intracellular and

Received 25 September 2013 **Returned for modification** 16 October 2013
Accepted 10 April 2014

Published ahead of print 28 April 2014

Address correspondence to Daniel D. Rockey, rockeyd@orst.edu.

* Present address: Kelsi M. Sandoz, Coxiella Pathogenesis Section, Laboratory of Intracellular Parasites, Rocky Mountain Laboratories, National Institute of Allergy and Infectious Diseases, National Institutes of Health, Hamilton, Montana, USA; Robert D. Allen III, Oregon Translational Research and Development Institute, Portland, Oregon, USA.

doi:10.1128/AAC.02064-13

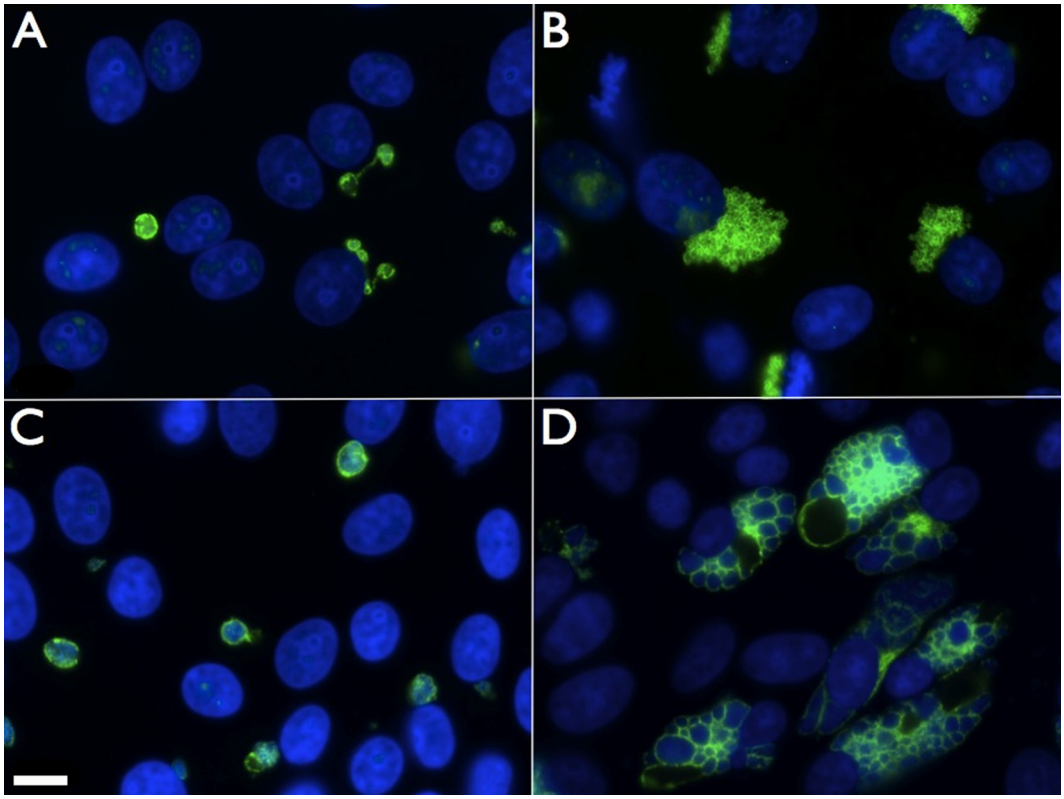

FIG 1 ST-669 treatment alters the size and structure of *C. caviae* inclusions. Immunofluorescence microscopy of ST-669 (A and C)- and DMSO (B and D)-treated *C. caviae*-infected Vero cells fixed at 20 h (A and B) or 40 h (C and D) postinfection was performed. Images were taken at ×100 magnification, and the scale bar in panel C indicates 10 μm for each panel. *C. caviae* inclusions were labeled with anti-IncA (green), and total DNA was labeled with DAPI (blue).

extracellular bacteria. The results demonstrate that ST-669 delays growth and development by chlamydiae and *Coxiella burnetii* and that a fluorescent derivative of the compound (ST-669F) localizes specifically to intracellular LDs.

MATERIALS AND METHODS

Reagents and antibodies. C6-NBD-ceramide (catalog no. N-1154), MitoTracker (catalog no. M-7512), and Texas Red dextran (catalog no. D-1864) were purchased from Invitrogen. Native ST-669 and its fluorescent derivative were purchased through SIGA Technologies (Corvallis, OR).

Cells infected with *Chlamydia* spp. or *Coxiella burnetii* were labeled with monoclonal or polyclonal primary antibodies specific to chlamydial lipopolysaccharide (LPS), *C. trachomatis* L2 IncA, *C. caviae* GPIC IncA, or a polyclonal antiserum against heat-fixed *Coxiella burnetii*. Appropriate species and isotype-specific secondary antibodies were purchased from Invitrogen. These secondary antibodies were tagged with either Alexa Fluor 488 (green) or Alexa Fluor 594 (red).

Host cells, chlamydial strains, and cultures. Three different cell lines were used for analysis in inhibition assays: McCoy (murine epithelial), HeLa (human endocervical), and Vero (African green monkey kidney). All cells were propagated in minimum essential medium supplemented with 10% fetal bovine serum (MEM-10). Chlamydial strains used for assays were *C. caviae* GPIC, *C. trachomatis* L2 434/Bu, and *C. muridarum* Weiss, and all were cultured in MEM-10 containing 10 μg of gentamicin/ml. All experiments with *Coxiella burnetii* used the avirulent Nine Mile phase II strain and were conducted with standard BSL-II practices (23).

Infections. Mammalian cells were plated in 24-well trays and incubated overnight to a confluence of 100%. Bacterial strains were inoculated onto cells at a multiplicity of infection (MOI) of 1. Inocula were suspended in MEM-10 containing 10 μM ST-669 or dimethyl sulfoxide (DMSO) and plated in 1-ml volumes. Plates were centrifuged at 2,000 rpm at 37°C for 1 h and then transferred to a 37°C incubator.

Quantification of bacterial genome copies from infected cell culture. McCoy (murine), Vero (primate), or HeLa (human) cells were plated in 24-well trays and incubated overnight to a confluence of 100%. Bacterial strains were suspended in MEM-10 and inoculated onto cells at an MOI of 0.5 to 1. Plates were centrifuged at 2,000 rpm at 37°C for 1 h and then transferred to a 37°C incubator. Infected cells were briefly sonicated to lyse and release bacteria. The lysates were collected in microcentrifuge tubes and stored at −20°C prior to analysis. DNA was extracted using a Qiagen DNeasy blood and tissue kit, using instructions provided by the manufacturer. The single exception to the described technique was the addition of 5 mM dithiothreitol to the initial lysis buffer. All TaqMan reagents for quantitative real-time PCR were purchased from Applied Biosystems, and TaqMan universal PCR Master mix was used with an input of 5 μl of template DNA and primers and probes with 5′-6FAM and a 3′-MGBNFQ labels. Primers and probes were specific to either *C. caviae* GPIC *ompA* (probe 6FAM-CATCACACCAAGT AGAGC-MGBNFQ), *C. trachomatis ompA* (F-CATGGTATCTCCGAGC TGACC, R-ACTGTCTTTGATGTTACCACTCTGAAC, and probe 6FAM-CTAGCTTTCACATCGCC-MGBNFQ), or *Coxiella burnetii dotA* (24). Tenfold serial dilutions of quantitated plasmid standards containing each target gene were included in the analyses at concentrations ranging from 10^9 to 10^3 genome copies per assay. Genome copy number and standard error were automatically calculated using an ABI StepOne real-time PCR machine with standard curve settings and extrapolated to reflect total copy number of bacteria per ml.

Immunofluorescence and cell structure labeling. (i) C6-NBD-ceramide and ST-669F. Vero cells were seeded onto coverslips at 30% confluence in MEM-10 and incubated overnight. Medium was aspirated and replaced with 500 μl of 10 μM C6-NBD-ceramide in phos-

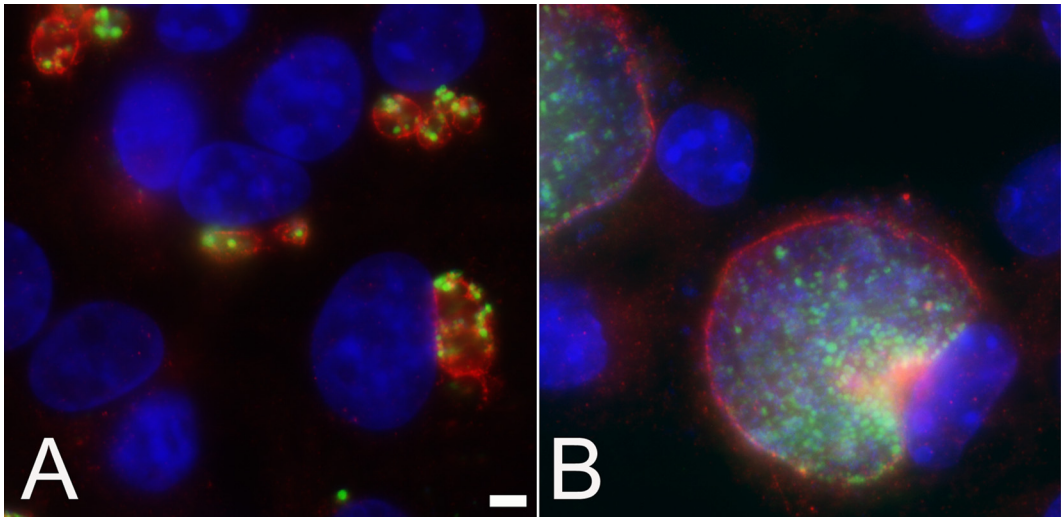

FIG 2 Treatment of *C. trachomatis*-infected Vero cells with ST-669 affects inclusion size and chlamydial abundance. Infected and treated Vero cells were fixed with methanol at 40 h postinfection. Fixed monolayers were labeled with anti-IncA (red), anti-MOMP (green), and DAPI for DNA (blue) and visualized using a ×100 objective lens. Infected cells were treated with either ST-669 (A) or the vehicle, DMSO (B). The scale bar in panel A indicates 5 μm for both panels.

phate-buffered saline (PBS). Plates were incubated for 1 h at 37°C, the C6-NBD-ceramide label was aspirated, and the cells were overlaid with MEM-10 and incubated at 37°C for an additional 2 h. Fresh medium containing 10 μM ST-669F was added onto cells, followed by incubation for 1 h. Medium was removed and replaced with PBS before mounting coverslips onto slides and examining cells on the fluorescence microscope. The C6-NBD-ceramide was visualized on the fluorescein channel and ST-669F was visualized on the DAPI (4′,6′-diamidino-2-phenylindole) channel.

(ii) MitoTracker and ST-669F. Vero cells were seeded onto coverslips in 24-well trays at a confluence of 30% and incubated overnight. Medium was removed and replaced with serum-free medium containing a mixture of 125 nM MitoTracker (Invitrogen) and 10 μM ST-669F, followed by incubation for 1 h. Medium was removed, the cells were washed with PBS, and coverslips were mounted to visualize on the microscope using the rhodamine (MitoTracker) or DAPI (ST-669F) channel.

(iii) Bodipy 493/503 and ST-669F. Vero, McCoy, or HeLa cells were seeded at a confluence of 30% onto coverslips in MEM-10 containing 100 μM oleic acid and then incubated overnight. Medium was removed and replaced with MEM-10 containing 1 μM Bodipy 493/503 and 10 μM ST-669F. Cells were incubated for 1 h at 37°C, washed with 1× PBS, and then mounted onto slides for microscopy. Images were visualized using the fluorescein (Bodipy 493/503) or DAPI (ST-669F) channel.

Immunofluorescence. Cells were plated onto 12-mm coverslips in 24-well trays, infected as described above, fixed with 100% methanol for 10 min, and washed twice with PBS. Fixed cells were labeled with specific antibodies, as indicated, followed by appropriate secondary antibodies conjugated with rhodamine or fluorescein fluorescent labels.

RESULTS AND DISCUSSION

ST-669 delays the growth of tested obligate intracellular bacteria. ST-669 is a novel antiviral compound that has a spectrum of activity across a wide range of different virus families (22). The present study was undertaken to examine whether ST-669 also has activity against intracellular bacteria, with a primary focus on chlamydiae and *Coxiella burnetii*. Treatment of infected primate-derived cells with 10 μM ST-669 slowed the growth of *C. trachomatis*, *C. caviae*, *C. muridarum*, and *Coxiella burnetii*. Markedly smaller inclusions (*C. caviae* [Fig. 1A and C], *C. trachomatis* [Fig. 2A]) or vacuoles (*Coxiella burnetii* [data not shown]) are seen in ST-669-treated wells, and there is a greater reduction in genome copies in ST-669-treated wells at later points during the infection (Fig. 3). Reduction of EB production in ST-669-treated *C. trachomatis* and *C. caviae*-infected Vero cells (not shown) were parallel with the reduction in genome copies, suggesting ST-669 is not bactericidal and that RB to EB transition occurs in the presence of ST-669. These results extend the spectrum of activity of ST-669 to include these intracellular bacteria and increase the possible therapeutic spectrum of ST-669 or derived compounds.

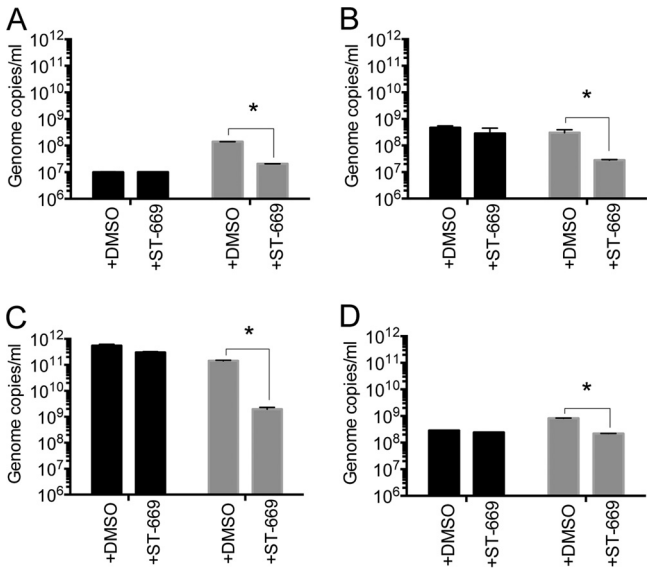

FIG 3 ST-669 inhibits growth of *Coxiella burnetii* and *Chlamydia* spp. in a host-specific manner. qPCR analyses of ST-669- and DMSO-treated *Coxiella burnetii* (A; 72 h postinfection), *C. muridarum* (B; 20 h postinfection), *C. trachomatis* L2 (C; 40 h postinfection), and *C. caviae* GPIC (D; 40 h postinfection) inside McCoy (black) or Vero (gray) cells. All experiments were conducted at an MOI of 1. Genome copies/ml are plotted on the *y* axis. The asterisk indicates statistically significant differences ($P < 0.0001$).

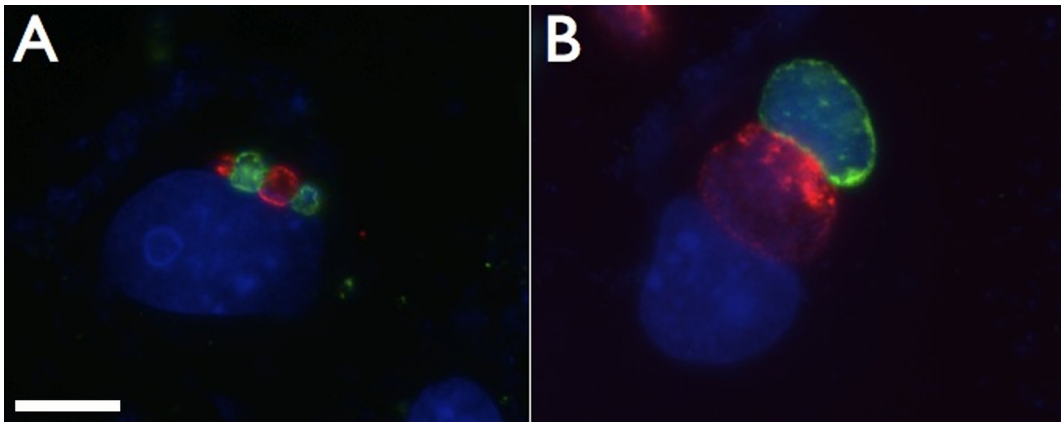

FIG 4 Coinfection of *C. caviae* and *C. trachomatis* demonstrate the altered inclusion phenotype of ST-669-treated *C. caviae*. Vero cells treated with 10 μM ST-669 were coinfected with *C. caviae* (green) and *C. trachomatis* (red), followed by incubation for 20 h (A) and 50 h (B). The cells were then fixed and labeled with species-specific anti-IncA antibodies. The total DNA was labeled with DAPI (blue). The scale bar in panel A indicates 10 μm for each panel.

Antibacterial activity of ST-669 activity is host species dependent. To determine whether the antibacterial activity of ST-669 is specific to certain host cell types, we cultured *C. caviae*, *C. muridarum*, *C. trachomatis*, and *Coxiella burnetii* in cells of murine (McCoy), primate (Vero), or human (HeLa) origin (Fig. 3). ST-669 was active in HeLa and Vero cell lines (HeLa data not shown). No inhibition of bacterial growth was observed in the McCoy cell lines (Fig. 3). These data demonstrate that the inhibitory activity of ST-669 is host cell specific, which is consistent with the antiviral properties of the compound.

***Chlamydia caviae* inclusion morphology within treated cells.** Typical development of *C. caviae* inclusions within any tested cell line results in multilobed inclusions that can be clearly visualized by staining with antibodies specific to the inclusion membrane protein IncA (Fig. 1B and D) (25). This is in contrast to inclusions formed by *C. trachomatis*, which are generally single inclusions containing many developmental forms. Treatment of *C. caviae*-infected Vero cells with ST-669 led to the formation of univacuolar inclusions, with chlamydiae localized to the cell in a single, round vesicle (Fig. 1A and C). This change remained consistent throughout the *C. caviae* developmental cycle. *C. caviae*-infected cells treated with ST-669 also contain IncA-laden empty vesicles (secondary inclusions; Fig. 1A) that are connected to the primary inclusion within the cell. Secondary inclusions linked to the primary inclusion by IncA-laden fiber-like structures are also observed in most strains of *C. trachomatis* grown in cell culture (26). Therefore, treatment of *C. caviae*-infected cells with ST-669 leads to alteration in inclusion structure that parallels the reduction in chlamydial genome copies and leads to inclusions that are similar to those formed by *C. trachomatis* (Fig. 4).

Cycloheximide is an inhibitor of host protein synthesis that has no effect on bacterial translation. This distinction allowed us to examine whether host protein synthesis was required for the activity of ST-669. An intermediate inclusion phenotype (Fig. 5C) and an intermediate number of chlamydial genome copies (Fig. 6) were observed in *C. caviae* GPIC-infected cells treated with both ST-669 and cycloheximide, and this effect was specific to HeLa and Vero cells (Fig. 6 and data not shown). This suggests that host protein synthesis is at least partially required for ST-669-mediated delay of bacterial growth and supports the hypothesis that the ST-669 mechanism of action is directed at a host process important for chlamydial replication or development within HeLa and Vero cell lines.

A fluorescent analog of ST-669 localizes to lipid droplets. A fluorescent fluorophore was conjugated to ST-669 and used to track localization of the molecule *in vitro*. This derivative compound (ST-669F) has demonstrable antiviral activity against vaccinia virus and *C. caviae* that is similar to that of the parental compound (data not shown). Fluorescent antibody images of ST-669F-treated cells show a distinct localization of the compound to round vesicular structures within the cytoplasm of the cell (Fig. 7 and 8). Double-label fluorescence microscopy with probes for in-

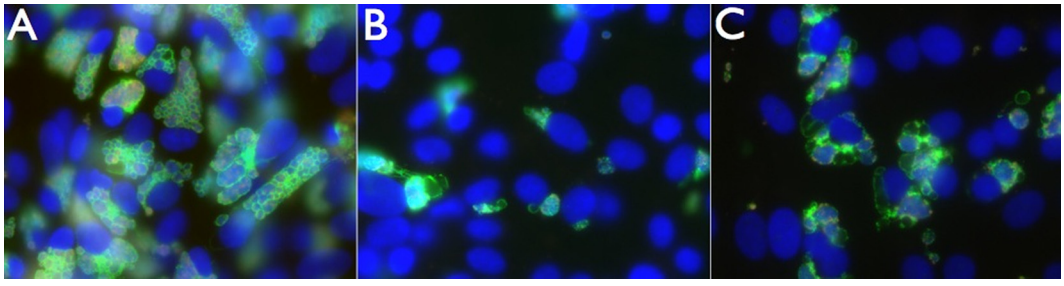

FIG 5 Cycloheximide and ST-669 cotreatment of *C. caviae*-infected cells. Vero cells were infected with *C. caviae* and treated with either DMSO plus cycloheximide (A), ST-669 (B), or ST-669 plus cycloheximide (C). The cells were then cultured for 40 h, fixed with methanol, and stained for immunofluorescence microscopy. Images were visualized for total DNA (blue), chlamydial LPS (red), and IncA (green), using the ×40 objective lens.

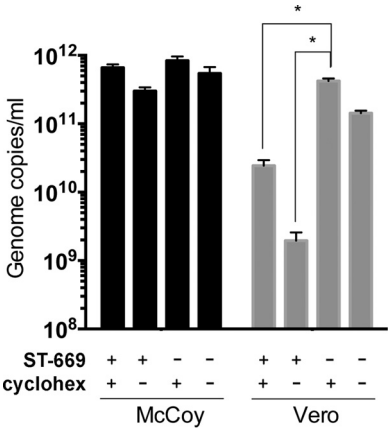

FIG 6 Cycloheximide treatment partially reverses the inhibitory effect of ST-669. qPCR of ST-669-treated or untreated (i.e., DMSO only) *C. trachomatis* L2-infected McCoy and Vero cells in the presence or absence of 100 μg of cycloheximide (cyclohex)/ml. Infections were sonicated, and gDNA was collected at 40 h postinfection before assay by qPCR. The asterisk indicates statistically significant differences ($P < 0.0001$).

dividual organelles in combination with ST-669F was used to determine subcellular compound localization. There was no colocalization of labels when cells were doubly labeled with ST-669F and markers that localize to lysosomes (Fig. 7A), mitochondria (Fig. 7B) or the Golgi apparatus (Fig. 7C). However, Bodipy 493/503, which targets phospholipids and LDs, and ST-669F colocalized very specifically within treated cells (Fig. 7D). This result supports the conclusion that ST-669F localizes to LDs within treated cells. ST-669F colocalizes with LD structures in McCoy, HeLa, and Vero cells (Fig. 8), even though antimicrobial activity is not evident in McCoy (murine) cells. Treatment of mammalian cells with oleic acid induces LD formation, leading to expanded numbers of intracellular LDs (25). Cells treated with oleic acid show an abundance of ST-669F-labeled structures that colocalize with Bodipy 493/503-labeled LDs (Fig. 8) in both McCoy and Vero cells. No obvious differences are noted in LD size or morphology in ST-669-treated cells, which is different from other chemical compounds that inhibit chlamydial growth by blocking LD formation (10).

The colocalization of fluorescent ST-669 with LDs supports a possible model in which ST-669 disrupts growth of both bacterial and viral organisms through an LD-mediated mechanism, by targeting a host LD-associated pathway that is specific to HeLa and Vero cells. A connection between lipid metabolism and ST-669 activity is also supported by the marked alteration in *C. caviae* inclusion structure in treated primate cells. This difference is evident very early in development and remains evident throughout the development of the pathogen.

It is also possible that ST-669 affects cells through processes

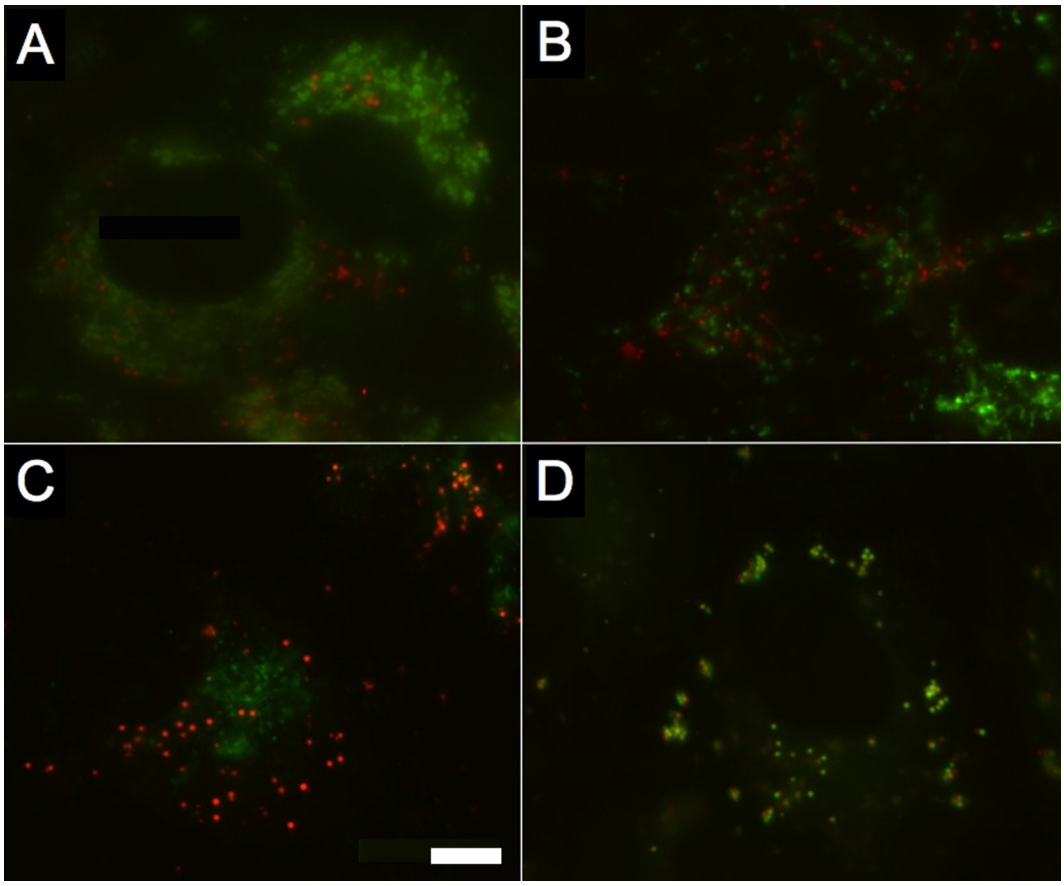

FIG 7 Dual labeling of host cell structures with ST-669F shows that ST-669F trafficks to intracellular lipid droplets. Uninfected Vero cells were labeled with ST-669F (red) and probes specific to different organelles (green) to determine colocalization of the ST-669F molecule. (A) Lysosomes; (B) mitochondria; (C) Golgi apparatus; (D) lipid droplets. The scale bar in panel C indicates 5 μm for each panel.

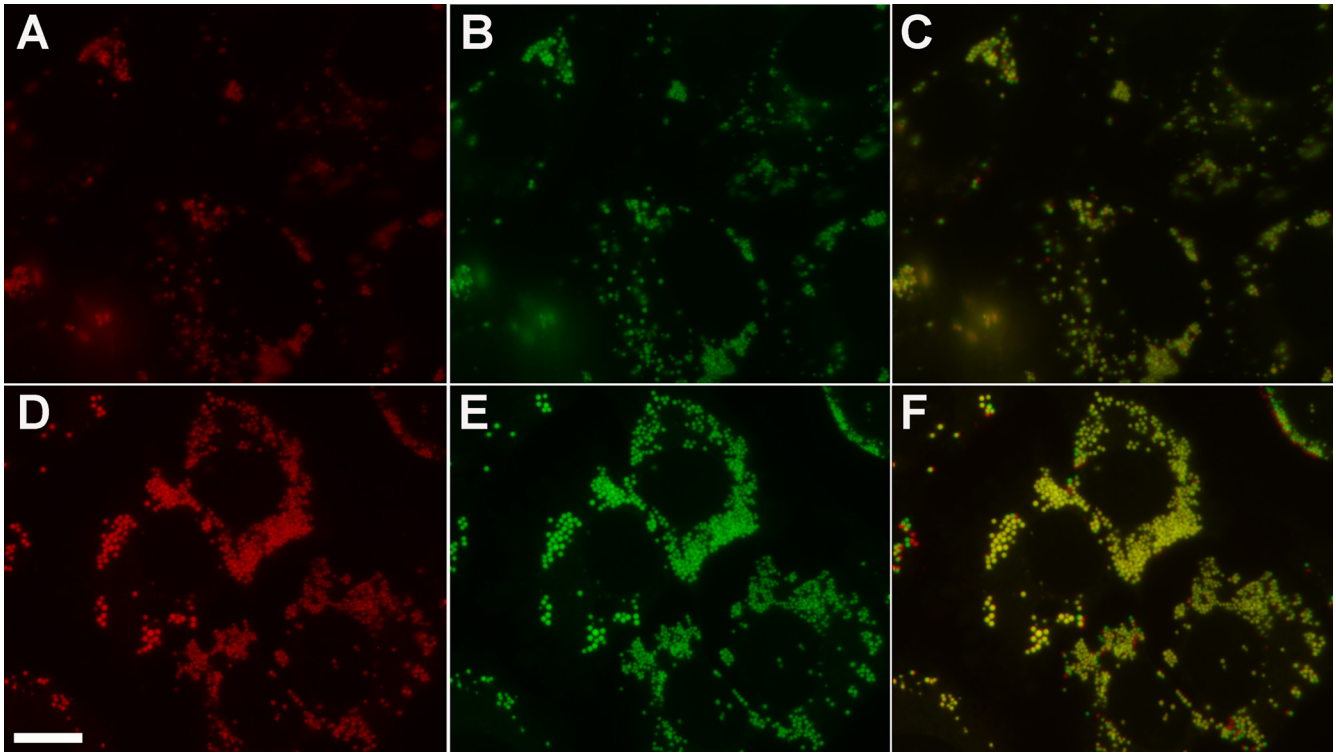

FIG 8 Colocalization of ST-669F and Bodipy 493/503 in both McCoy and Vero cells treated with oleic acid. Uninfected McCoy cells (top row) and Vero cells (bottom row) were treated with 100 μM oleic acid for 16 h and then labeled with a combination of ST-669F (green) and Bodipy 493/503 (red) to determine colocalization of the ST-669F molecule. Bodipy 493/503 and ST-669F were added to the culture medium as indicated in Materials and Methods, and then the cells were visualized for each label. (A and D) Bodipy 493/503-labeled lipid droplets; (B and E) ST-669F, pseudocolored green; (C and F) merged image of each of the two panels.

independent of LD biology and that the localization of the fluorescent ST-669 compound to LDs is not directly associated with its anti-infective activity. The work by Roshick et al. has demonstrated that innate antichlamydial immune effectors function differently in murine and primate cell types (27), and some aspect of these primate-specific pathways may be uniquely affected by ST-669. Work addressing the specific mechanism of action of ST-669 and its antimicrobial spectrum continues in our laboratories.

ACKNOWLEDGMENTS

We thank Amy Moore, Erin Brown, and Robert Jordan at SIGA technologies who provided ongoing technical support throughout the study. Valerie Elias at Oregon State University provided excellent technical work in support of this project. We thank Aleksandra Sikora, Erik Cram, and Tim Putman for critical reading of the manuscript.

The Rockey laboratory received support for this work from grants AI088540-02 and AI086469-01 from the National Institutes of Health.

REFERENCES

1. **Starnbach MN, Roan NR.** 2008. Conquering sexually transmitted diseases. Nat. Rev. Immunol. **8:**313–317. http://dx.doi.org/10.1038/nri2272.
2. **Abdelrahman YM, Belland RJ.** 2005. The chlamydial developmental cycle. FEMS Microbiol. Rev. **29:**949–959. http://dx.doi.org/10.1016/j.femsre.2005.03.002.
3. **Carabeo RA, Mead DJ, Hackstadt T.** 2003. Golgi-dependent transport of cholesterol to the *Chlamydia trachomatis* inclusion. Proc. Natl. Acad. Sci. U. S. A. **100:**6771–6776. http://dx.doi.org/10.1073/pnas.1131289100.
4. **Hatch GM, McClarty G.** 1998. Phospholipid composition of purified *Chlamydia trachomatis* mimics that of the eucaryotic host cell. Infect. Immun. **66:**3727–3735.
5. **Moore ER, Fischer ER, Mead DJ, Hackstadt T.** 2008. The chlamydial inclusion preferentially intercepts basolaterally directed sphingomyelin-containing exocytic vacuoles. Traffic **9:**2130–2140. http://dx.doi.org/10.1111/j.1600-0854.2008.00828.x.
6. **Hackstadt T, Rockey DD, Heinzen RA, Scidmore MA.** 1996. *Chlamydia trachomatis* interrupts an exocytic pathway to acquire endogenously synthesized sphingomyelin in transit from the Golgi apparatus to the plasma membrane. EMBO J. **15:**964–977.
7. **Hackstadt T, Scidmore MA, Rockey DD.** 1995. Lipid metabolism in *Chlamydia trachomatis*-infected cells: directed trafficking of Golgi-derived sphingolipids to the chlamydial inclusion. Proc. Natl. Acad. Sci. U. S. A. **92:**4877–4881. http://dx.doi.org/10.1073/pnas.92.11.4877.
8. **Scidmore MA, Fischer ER, Hackstadt T.** 1996. Sphingolipids and glycoproteins are differentially trafficked to the *Chlamydia trachomatis* inclusion. J. Cell Biol. **134:**363–374. http://dx.doi.org/10.1083/jcb.134.2.363.
9. **Wolf K, Hackstadt T.** 2001. Sphingomyelin trafficking in *Chlamydia pneumoniae*-infected cells. Cell. Microbiol. **3:**145–152. http://dx.doi.org/10.1046/j.1462-5822.2001.00098.x.
10. **Kumar Y, Cocchiaro J, Valdivia RH.** 2006. The obligate intracellular pathogen *Chlamydia trachomatis* targets host lipid droplets. Curr. Biol. **16:**1646–1651. http://dx.doi.org/10.1016/j.cub.2006.06.060.
11. **Cocchiaro JL, Kumar Y, Fischer ER, Hackstadt T, Valdivia RH.** 2008. Cytoplasmic lipid droplets are translocated into the lumen of the *Chlamydia trachomatis* parasitophorous vacuole. Proc. Natl. Acad. Sci. U. S. A. **105:**9379–9384. http://dx.doi.org/10.1073/pnas.0712241105.
12. **Bartz R, Zehmer JK, Zhu M, Chen Y, Serrero G, Zhao Y, Liu P.** 2007. Dynamic activity of lipid droplets: protein phosphorylation and GTP-mediated protein translocation. J. Proteome Res. **6:**3256–3265. http://dx.doi.org/10.1021/pr070158j.
13. **Beller M, Thiel K, Thul PJ, Jackle H.** 2010. Lipid droplets: a dynamic organelle moves into focus. FEBS Lett. **584:**2176–2182. http://dx.doi.org/10.1016/j.febslet.2010.03.022.
14. **Digel M, Ehehalt R, Fullekrug J.** 2010. Lipid droplets lighting up: insights from live microscopy. FEBS Lett. **584:**2168–2175. http://dx.doi.org/10.1016/j.febslet.2010.03.035.

15. **Martin S, Parton RG.** 2006. Lipid droplets: a unified view of a dynamic organelle. Nat. Rev. Mol. Cell. Biol. **7:**373–378. http://dx.doi.org/10.1038/nrm1912.
16. **van der Meer-Janssen YP, van Galen J, Batenburg JJ, Helms JB.** 2010. Lipids in host-pathogen interactions: pathogens exploit the complexity of the host cell lipidome. Prog. Lipid Res. **49:**1–26. http://dx.doi.org/10.1016/j.plipres.2009.07.003.
17. **Alvisi G, Madan V, Bartenschlager R.** 2011. Hepatitis C virus and host cell lipids: an intimate connection. RNA Biol. **8:**258–269.
18. **Heaton NS, Randall G.** 2010. Dengue virus-induced autophagy regulates lipid metabolism. Cell Host Microbe **8:**422–432. http://dx.doi.org/10.1016/j.chom.2010.10.006.
19. **Cheung W, Gill M, Esposito A, Kaminski CF, Courousse N, Chwetzoff S, Trugnan G, Keshavan N, Lever A, Desselberger U.** 2010. Rotaviruses associate with cellular lipid droplet components to replicate in viroplasms, and compounds disrupting or blocking lipid droplets inhibit viroplasm formation and viral replication. J. Virol. **84:**6782–6798. http://dx.doi.org/10.1128/JVI.01757-09.
20. **Unterstab G, Gosert R, Leuenberger D, Lorentz P, Rinaldo CH, Hirsch HH.** 2010. The polyomavirus BK agnoprotein colocalizes with lipid droplets. Virology **399:**322–331. http://dx.doi.org/10.1016/j.virol.2010.01.011.
21. **Flaspohler JA, Jensen BC, Saveria T, Kifer CT, Parsons M.** 2010. A novel protein kinase localized to lipid droplets is required for droplet biogenesis in trypanosomes. Eukaryot. Cell **9:**1702–1710. http://dx.doi.org/10.1128/EC.00106-10.
22. **Burgeson JR, Moore AL, Boutilier JK, Cerruti NR, Gharaibeh DN, Lovejoy CE, Amberg SM, Hruby DE, Tyavanagimatt SR, Allen RD, III, Dai D.** 2012. SAR analysis of a series of acylthiourea derivatives possessing broad-spectrum antiviral activity. Bioorg. Med. Chem. Lett. **22:**4263–4272. http://dx.doi.org/10.1016/j.bmcl.2012.05.035.
23. **Hackstadt T.** 1996. Biosafety concerns and *Coxiella burnetii*. Trends Microbiol. **4:**341–342. http://dx.doi.org/10.1016/0966-842X(96)81555-1.
24. **Howe D, Heinzen RA.** 2006. *Coxiella burnetii* inhabits a cholesterol-rich vacuole and influences cellular cholesterol metabolism. Cell Microbiol. **8:**496–507. http://dx.doi.org/10.1111/j.1462-5822.2005.00641.x.
25. **Rockey DD, Fischer ER, Hackstadt T.** 1996. Temporal analysis of the developing *Chlamydia psittaci* inclusion by use of fluorescence and electron microscopy. Infect. Immun. **64:**4269–4278.
26. **Suchland RJ, Rockey DD, Weeks SK, Alzhanov DT, Stamm WE.** 2005. Development of secondary inclusions in cells infected by *Chlamydia trachomatis*. Infect. Immun. **73:**3954–3962. http://dx.doi.org/10.1128/IAI.73.7.3954-3962.2005.
27. **Roshick C, Wood H, Caldwell HD, McClarty G.** 2006. Comparison of gamma interferon-mediated antichlamydial defense mechanisms in human and mouse cells. Infect. Immun. **74:**225–238. http://dx.doi.org/10.1128/IAI.74.1.225-238.2006.